Journal of the Ceramic Society of Japan 118 [8] 726-730 2010 Paper

Electric-field-induced strain for $(Bi_{1/2}Na_{1/2})TiO_3$-based lead-free multilayer actuator

Hajime NAGATA,† Yuji HIRUMA and Tadashi TAKENAKA

Department of Electrical Engineering, Faculty of Science and Technology, Tokyo University of Science, 2641 Yamazaki, Noda, Chiba 278–8510

Multilayer prototype actuators were demonstrated using $(Bi_{1/2}Na_{1/2})TiO_3$ [BNT]-based ceramics as active layers and Pt as internal electrodes. One of the BNT-based solid solutions, $0.68(Bi_{1/2}Na_{1/2})TiO_3$–$0.04(Bi_{1/2}Li_{1/2})TiO_3$–$0.28(Bi_{1/2}K_{1/2})TiO_3$ (BNLKT4–28) has been selected as the an active layer and it showed a relatively large piezoelectric strain constant d_{33} of 130 pC/N and a high depolarization temperature T_d of 226°C. The total number of layers was 10 and the active layer thickness was 125 μm for the sintered body. The final compact dimensions were approximately 5 × 5 × 2 mm^3. From the SEM observation, there were no apparent delaminations around the interface between Pt electrodes and active BNLKT layers. The large electric-field-induced strain at 70 kV/cm was 0.17% and the longitudinal dynamic displacement at the same electric field was 2.1 μm.

Key-words : Lead-free, Multilayer ceramic actuator, Electric-field-induced strain, Bismuth sodium titanate

[Received May 6, 2010; Accepted July 15, 2010]

1. Introduction

Piezoelectric materials play an important role in electrical devices, such as actuators, accelerators, piezoelectric motors, transducers, filters, and resonators. Most piezoelectric devices are composed of $Pb(Zr,Ti)O_3$ (PZT)-based piezoelectric ceramics because of their excellent piezoelectric properties.[1),2)] However, PZT ceramics contain a large amount of PbO; therefore, lead-free piezoelectric materials used to replace PZT have recently been required from the viewpoint of environmental protection. In particular, actuator applications have a large market in piezoelectric devices; thus, the development of lead-free piezoelectric materials is strongly demanded in the actuator field. As the lead-free piezoelectric candidates for actuators, various perovskite-structured ferroelectrics, such as $BaTiO_3$ (BT), $(Bi_{1/2}K_{1/2})TiO_3$ (BKT), $(K,Na)NbO_3$ (KNN), and $(Bi_{1/2}Na_{1/2})TiO_3$ (BNT)-based solid solutions, have recently been actively studied.[3)–23)] In particular, KNN-based ceramics, such as textured LF4,[6)] are expected to be the best material for lead-free actuators owing to their excellent piezoelectric strain constant d_{33} of ~400 pC/N. Moreover, KNN-based multilayer piezoelectric ceramics with nickel inner electrodes have been developed, and they exhibited a large electric-field-induced strain.[24)] On the other hand, raw materials, such as Nb_2O_5 and K_2CO_3, are very expensive compared with PZT-based materials, and their processing cost is also high owing to the difficulties and complications in their manufacturing process. Therefore, the economical issue may be a stumbling block in the progress of the practical application of KNN based materials in actuators.

BNT ceramics are expected to be one of the superior candidates for lead-free piezoelectric materials owing to their friendly for current manufacturing process, low material cost, and relatively high piezoelectric properties.[13)–23)] However, these ceramics exhibit a high coercive field ($E_c = 73$ kV/cm), resulting in problems in the poling process. Therefore, BNT has been modified using many materials, such as $BaTiO_3$ (BT),[3),15)] $KNbO_3$ (KN),[33)] $(Bi_{1/2}K_{1/2})TiO_3$ (BKT).[16),25),26)] All of these solid solutions show improved piezoelectric properties and easy treatment of the poling process by such modification as compared with pure BNT ceramics. However, the d_{33} values of these materials are still not as large as these of PZT- and KNN-based materials. To cover the low d_{33} values of BNT-based materials, it is generally considered that a multilayer structure is very effective for actuator applications because the total displacement can be increased proportionally to the layer number of the multilayer structure. However, there have been no reports on the multilayer structure of BNT-based ceramics. In this study, a prototype of the multilayer structure was prepared using BNT-based materials and Pt inner electrodes.

Selecting the BNT-based composition, we took into account the working temperature range. The crystal structure of BNT is rhombohedral at RT, and the rhombohedral-tetragonal phase transition temperature $T_{R\text{-}T}$ and the Curie temperature T_C are approximately 300 and 540°C on heating, respectively, for a BNT single crystal.[27)–29)] In addition, BNT has a depolarization temperature T_d of approximately 185°C. Although it has been reported that T_d is the phase transition temperature between ferroelectric and antiferroelectric phases,[30)] the nature of the phase transition is not yet clear. Moreover, the working temperature is limited by T_d; thus, is very important for practical applications. Recently, we have reported that $x(Bi_{1/2}Na_{1/2})TiO_3$–$y(Bi_{1/2}Li_{1/2})TiO_3$–$z(Bi_{1/2}K_{1/2})TiO_3$, [BNLKT100y–100z ($x + y + z = 1$)] solid solution shows relatively high T_d values of higher than 200°C and a relatively large d_{33} of 150 pC/N.[31),32)] Note again that the displacement can be enlarged by increasing the layer number of the multilayer structure; however T_d is a material characteristic that is difficult to control extrinsically. In this study, multilayer piezoelectric ceramics were demonstrated using the BNLKT4–28 composition for the active piezoelectric layer to see the stability of multilayer structure, phase transition temperature and strain behavior.

† Corresponding author: H. Nagata; E-mail: nagata@takenaka.ee.noda.tus.ac.jp

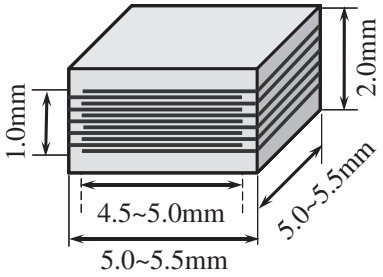

Fig. 1. Schematic diagram of green compact.

2. Experimental procedure

BNKLT ceramics were prepared by a conventional ceramic fabrication technique. Reagent-grade metal oxide or carbonate powders of Bi_2O_3, TiO_2, Na_2CO_3, K_2CO_3, and Li_2CO_3 were used as starting materials. Starting raw materials were mixed in ethanol with stabilized zirconia balls by ball milling for 24 h. After drying, the mixed powders were calcined at 800°C for 4 h. The calcined powders were ground again by ball milling for 6 h. The particle sizes of the milled powders were controlled to be 1–2 μm. The slurries for tape casting were prepared by mixing the calcined powders, solvent, binder and plasticizer. As inner electrodes, platinum paste (ML-3822, Shoei Chemical Inc.) was screen-printed on the sheet. Each sheet was laminated and cut to form the green compact shown in **Fig. 1**. The final dimensions of the green compact were about $5.5 \times 5.5 \times 2.0\,mm^3$. The total number of layers was 10 and the active layer thickness was about 100 μm for the sintered body. The green compact was heated to remove organic components and then sintered at 1120°C for 2 h. The calcined and ball-milled powders were also pressed into bulk pellets, and the pellets were sintered at 1120°C for 2 h in air for comparison with multilayer samples.

The crystal structures and lattice constants of the sintered bulk ceramics were confirmed by X-ray powder diffraction analysis using an X-ray diffractometer (Rigaku; RINT2000, Cu Kα). Microstructures were observed by scanning electron microscopy (SEM, Hitachi S-2400). Fired-on silver was used as electrodes connected to each inner electrode for the measurement of electrical properties. Resistivities were measured using a high resistance meter (YHP 4339B). The temperature dependences of the dielectric properties were measured using an automated dielectric measurement system with a multifrequency *LCR* meter (YHP 4275A and Wayne Kerr 6440B) at 1 k–1 MHz. Electric-field-induced strains were measured with unipolar driving at 0.1 Hz using a contact-type displacement sensor (Millitron Model 1240). The normalized d_{33}* is defined as follows.

$$d_{33}^{*}\ [\mathrm{pm/V}] = \frac{S\ [\%]}{E\ [\mathrm{kV/cm}]} \times 10^5 \qquad (1)$$

The bulk specimens for the measurement of piezoelectric properties were poled in a silicone oil bath at RT by applying a 5 kV/mm DC electric field for 5 min. After poling, k_{33} was determined by a resonance-antiresonance method using an impedance analyzer (Agilent 4294A). The free permittivity ε_{33}^{T} was determined from the capacitance at 1 kHz of the poled specimen. The elastic constants s_{33}^{E} were calculated from the frequency constant N_{33} and the measured density, ρ_0. Finally, the piezoelectric constants d_{33} were calculated from k_{33}, ε_{33}^{T} and s_{33}^{E} using,

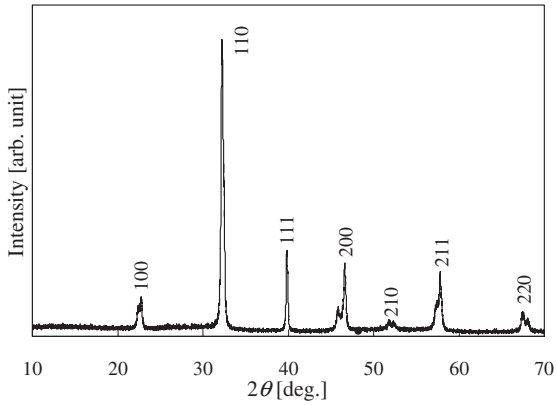

Fig. 2. X-ray diffraction pattern for BNLKT4–28.

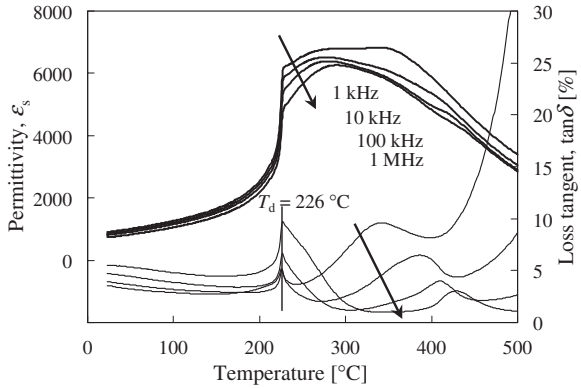

Fig. 3. Temperature dependences of dielectric constant ε_s and loss tangent $\tan\delta$ for poled BNLKT4–28.

$$d_{33} = k_{33}\sqrt{\varepsilon_{33}^{T} \cdot s_{33}^{E}} \qquad (2)$$

3. Results and discussion

3.1 Bulk characteristics of BNLKT4–28 ceramics

Figure 2 shows an X-ray diffraction (XRD) pattern for a BNLKT4–28 ceramic showing a single phase of a perovskite structure with tetragonal symmetry. The lattice constants calculated from the XRD pattern were $a = 3.895$ and $c = 3.928$ Å, and the lattice anisotropy (tetragonality) c/a was 1.0085. This anisotropy is relatively large and approximately the same as that in $BaTiO_3$. The relative density of the bulk sample sintered at 1120°C for 2 h is higher than 96%. The volume resisitivity ρ of bulk BNLKT4–28 is about $5 \times 10^{12}\,\Omega$·cm. **Figure 3** shows the temperature dependences of the dielectric properties ε_s and loss tangent $\tan\delta$ of bulk BNLKT4–28. The depolarization temperature, T_d, was determined to be 226°C from the peaks of $\tan\delta$. This temperature is consistent with that determined from the temperature dependences of piezoelectric properties. **Figure 4** shows the frequency dependence of the impedance Z of the (33) mode for BNLKT4–28. The electromechanical coupling factor k_{33} is 0.45, and the calculated piezoelectric strain constant d_{33} is 130 pC/N. From the measurement of the electric-field-induced strain S for the bulk sample, the normalized d_{33}* value was calculated to be 218 pm/V at 80 kV/cm using formula (1). The d_{33}* value is about 1.6-fold as large as the d_{33} value determined from the resonance and antiresonance method. Generally, the electric-field-induced strain consists of intrinsic and extrinsic effects. The intrinsic effect is due to the deformation of the

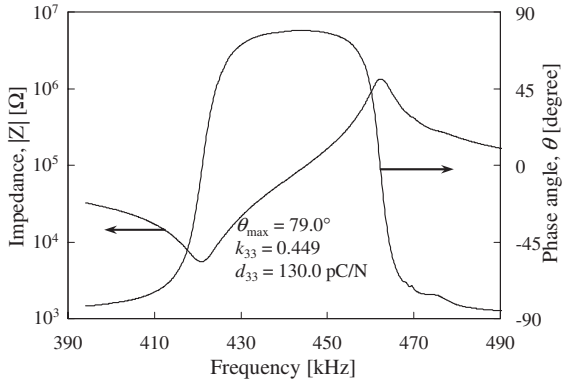

Fig. 4. Frequency dependence of impedance Z for bulk BNLKT4–28 in (33) mode.

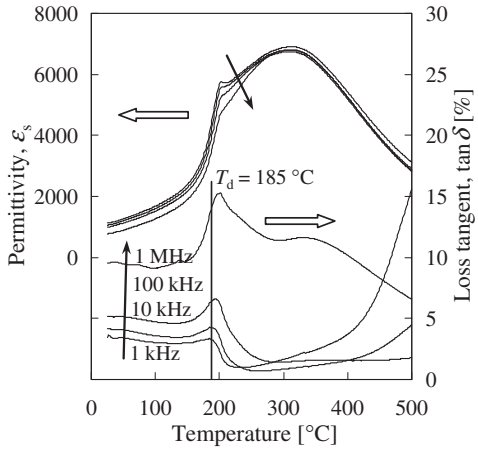

Fig. 6. Temperature dependences of dielectric constant ε_s and loss tangent $\tan\delta$ for multilayered BNLKT4–28.

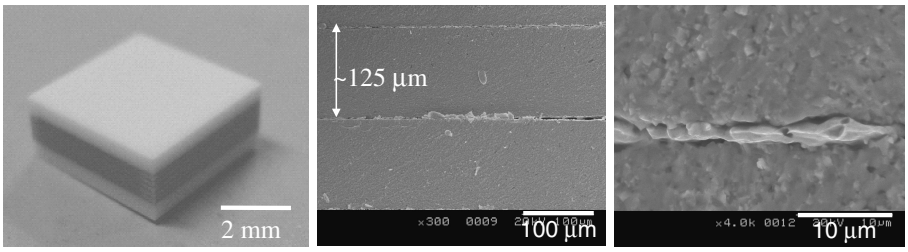

Fig. 5. Images of (a) external view and (b), (c) SEM micrographs.

crystal lattices by the electric-field. The d_{33} values obtained by the resonance technique correspond to the intrinsic effect. On the other hand, the differences between d_{33}* and d_{33} are associated with the extrinsic effects. Masuda analyzed the electric-field-induced strain of modified PZT as a superimposition of piezostriction (intrinsic effect) and electrostriction (extrinsic effect), where the electrostriction was mainly caused by the domain contribution.[34] Also, Tsurumi confirmed experimentally, by in situ XRD analysis, that the electric-field-induced strains of tetragonal PZT ceramics were composed of strain due to the intrinsic piezoelectric and extrinsic effects from 90° domain-wall motions.[35),36] The electric-field-induced phase transformation is also involved in the extrinsic effect, but BNLKT4–28 has no phase transition at room temperature.[31),32] Therefore, in the case of BNLKT4–28 ceramics with tetragonal symmetry, the origins of these differences between d_{33}* and d_{33} seem to be the 90° domain-wall motions.

3.2 Multilayer characteristics

Figure 5 shows the images of (a) the external view and (b), (c) SEM micrographs after the co-firing of multilayered BNLKT4–28 at 1120°C for 2 h. We could not observe the apparent bending of the sample in the external view. From SEM micrograph (b), the active layer thickness between electrodes was estimated to be approximately 125 μm for the sintered body. The average active layer thickness was calculated from some layer thicknesses in the SEM images to be 124.4 μm, and is used for the calculation of the dielectric constant ε_r and resisitivity ρ of the multilayered samples. SEM micrograph (c) indicates a homogeneous microstructure of active BNLKT layers with grain sizes of 1–2 μm. In SEM micrograph (c), the interface between BNLKT and the Pt electrode is clearly distinguished and there are no significant signs of reaction or diffusion between them. On the other hand, the adhesion between them appears relatively weak, but there are no measured data about this at present.

The ρ values of all co-fired samples are about $10^{10}\,\Omega$·cm on average. This value is 2 orders of magnitude lower than that of bulk ceramics. Anyhow, the ρ value of $10^{10}\,\Omega$·cm is sufficiently to apply a high DC electric field to the sample for *S–E* measurement. **Figure 6** shows the temperature dependences of the dielectric constant ε_r and loss tangent, $\tan\delta$ for the multilayer sample. The ε_r of the multilayer sample at RT is almost the same as that of the bulk ceramic. However, the T_d of 185°C for the multilayered sample is lower than that of the bulk ceramic. Some possible reasons for the T_d difference between the bulk and multilayered samples can be considered; one is the induced stress in the multilayer structure and another is the compositional variation. For example, in the case of $BaTiO_3$ (BT) thin films, Yanase et al. reported that the Curie temperature T_C was increased by the large lattice misfit strain in the heteroepitaxial BT films on $SrRuO_3$.[37] Therefore, it is considered that the phase transition temperature can be changed by an induced stress. On the other hand, Nakano et al., revealed the residual stress in BT-based multilayer ceramic capacitors (MLCCs) and the temperature dependences of their dielectric properties, indicating the absence of a significant shift in T_C with increasing residual stress up to about 200 MPa.[38),39] From those reports, it is considered that the effect of an induced stress has a small contribution to the T_d difference between the bulk and multilayered samples; however, it has not yet been clarified in the case of BNT-based ceramics so far. By considering the second possible reason (i.e. compositional variation), T_d was observed to markedly decrease with decreasing $(Bi_{1/2}K_{1/2})TiO_3$ content in the BNLKT system.[31),32] Therefore, it is speculated that the evaporation of Bi and K ions during baking and firing strongly affects the decrease in T_d in the multilayered samples. The reduction in resistivity in

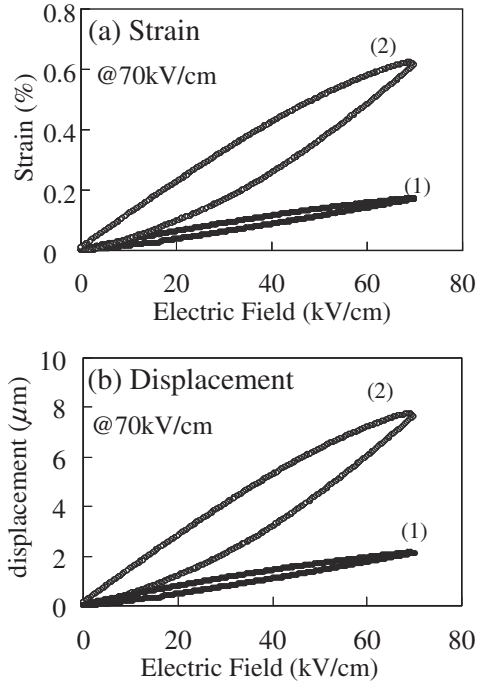

Fig. 7. (a) Electric-field-induced strain S and (b) displacement under unipolar driving at 70 kV/cm, (1) before and (2) after applying 80 kV/cm.

the multilayered samples seems to support the idea of the evaporation of Bi and K ions.

Figure 7(a)-(1) shows the electric-field-induced strain S under unipolar driving at 70 kV/cm. A large electric-field-induced strain of 0.17% at 70 kV/cm was obtained before applying 80 kV/cm, and the longitudinal dynamic displacement at the same electric field shown in Fig. 7(b)-(1) was 2.1 μm. The normalized d_{33}* was calculated to be 248 pm/V, which is similar to that in the bulk samples. This result indicates that our BNT-based multilayered prototype efficiently functioned under the unipolar driving up to 70 kV/cm. However, upon the application of a the high electric field of 80 kV/cm, both strain and displacement reached the extremely high values of 0.62% and 7.74 μm, respectively, at 70 kV/cm. The d_{33}* at that time was about 850 pm/V, which was extraordinarily large, as we expected. To understand this behavior, the S–E curve was measured using a single-layer specimen prepared from a multilayer sample. The single-layer specimen of 125 μm thickness also indicated a large d_{33}* of about 3000 pm/V at 80 kV/cm. This is obviously due not to the longitudinal piezoelectric and electrostrictive effects but to the bending effect. From this result, it is speculated that the large d_{33}* (~850 pm/V) in the 10-layer specimen is also suspected due to the bending effect after applying 80 kV/cm. In other words, certain interfaces between Pt electrodes and piezoelectric active layers were delaminated by an induced high electric field at 80 kV/cm, and then, the piezoelectric active layers were partially bend similarly to a Moonie structure[40),41)] and a tailor-made multilayer piezoelectric actuator.[42),43)]

4. Summary

A lead-free multilayer actuator was demonstrated using a bismuth sodium titanate, $(Bi_{1/2}Na_{1/2})TiO_3$ [BNT], -based solid solution [$x(Bi_{1/2}Na_{1/2})TiO_3$–$y(Bi_{1/2}Li_{1/2})TiO_3$–$z(Bi_{1/2}K_{1/2})TiO_3$, (BNLKT100y–100z, BNLKT4–28)] and Pt internal electrodes in this study. The bulk BNLKT4–28 shows a relatively large piezoelectric strain constant d_{33} of 130 pC/N and high depolarization temperature T_d of 226°C. In the prototype multilayer structure, the total number of layers was 10 and the active layer thickness was 125 μm for the sintered body. The final compact dimensions were approximately $5 \times 5 \times 2$ mm^3. From the SEM observation, we could not observe any apparent delamination around the interface between Pt electrodes and active BNLKT layers. The large electric-field-induced strain S at 70 kV/cm was 0.17% and the longitudinal dynamic displacement at the same electric field was 2.1 μm. Our demonstration of a BNT-based multilayered prototype was successful and showed a large displacement under unipolar driving up to 70 kV/cm.

Acknowledgments We are very grateful to Dr. M. Furukawa, Mr. D. Tanaka and Mr. K. Teranishi of TDK Corporation for providing us with tape-casting sheets and their lamination for multilayered green compacts.

References

1) B. Jaffe, R. S. Roth and S. Marzullo, *J. Appl. Phys.*, **25**, 809–810 (1954).
2) T. Yamamoto, *Jpn. J. Appl. Phys., Part 1*, **35**, 5104–5108 (1996).
3) H. Takahashi, Y. Numamoto, J. Tani and S. Tsurekawa, *Jpn. J. Appl. Phys., Part 1*, **45**, 7405–7408 (2006).
4) T. Karaki, K. Yan, T. Miyamoto and M. Adachi, *Jpn. J. Appl. Phys., Part 2*, **46**, L97–L98 (2007).
5) Y. Hiruma, R. Aoyagi, H. Nagata and T. Takenaka, *Jpn. J. Appl. Phys., Part 1*, **43**, 7556–7559 (2004).
6) Y. Saito, H. Takao, T. Tani, T. Nonoyama, K. Takatori, T. Homma, T. Nagaya and M. Nakamura, *Nature (London, U.K.)*, **432**, 84–87 (2004).
7) Y. P. Guo, K. Kakimoto and H. Ohsato, *Appl. Phys. Lett.*, **85**, 4121–4123 (2004).
8) M. Matsubara, T. Yamaguchi, W. Sakamoto, K. Kikuta, T. Yogo and S. Hirano, *J. Am. Ceram. Soc.*, **88**, 1190–1196 (2005).
9) H. Birol, D. Damjanovic and N. Setter, *J. Am. Ceram. Soc.*, **88**, 1754–1759 (2005).
10) K. Matsumoto, Y. Hiruma, H. Nagata and T. Takenaka, *Jpn. J. Appl. Phys., Part 1*, **45**, 4479–4483 (2006).
11) Z. F. Li, C. L. Wang, W. L. Zhong, J. C. Li and M. L. Zhao, *J. Appl. Phys.*, **94**, 2548–2552 (2003).
12) Y. Hiruma, R. Aoyagi, H. Nagata and T. Takenaka, *Jpn. J. Appl. Phys., Part 1*, **44**, 5040–5044 (2005).
13) H. Nagata, T. Shinya, Y. Hiruma, T. Takenaka, I. Sakaguchi and H. Haneda, *Ceram. Trans.*, **167**, 213–221 (2005).
14) A. Herabut and A. Safari, *J. Am. Ceram. Soc.*, **80**, 2954–2958 (1997).
15) T. Takenaka, K. Maruyama and K. Sakata, *Jpn. J. Appl. Phys., Part 1*, **30**, 2236–2239 (1991).
16) A. Sasaki, T. Chiba, Y. Mamiya and E. Otsuki, *Jpn. J. Appl. Phys., Part 1*, **38**, 5564–5567 (1999).
17) B. J. Chu, D. R. Chen, G. R. Li and Q. R. Yin, *J. Eur. Ceram. Soc.*, **22**, 2115–2121 (2002).
18) H. Nagata, M. Yoshida, Y. Makiuchi and T. Takenaka, *Jpn. J. Appl. Phys., Part 1*, **42**, 7401–7403 (2003).
19) X. X. Wang, X. G. Tang and H. L. W. Chan, *Appl. Phys. Lett.*, **85**, 91–93 (2004).
20) Y. Hiruma, Y. Makiuchi, R. Aoyagi, H. Nagata and T. Takenaka, *Ceram. Trans.*, **174**, 139–146 (2005).
21) Y. Hiruma, H. Nagata and T. Takenaka, *Jpn. J. Appl. Phys., Part 1*, **45**, 7409–7412 (2006).
22) D. Lin, D. Xiao, J. Zhu and P. Yu, *Appl. Phys. Lett.*, **88**, 062901 (2006).

23) S. Zhang, T. R. Shrout, H. Nagata, Y. Hiruma and T. Takenaka, *IEEE Trans. Ultrason. Ferroelectr. Freq. Control*, 54, 910–917 (2007).
24) S. Kawada, M. Kimura, Y. Higuchi and H. Takagi, *Appl. Phys. Express*, 2, 111401 (2009).
25) M. Izumi, K. Yamamoto, M. Suzuki, Y. Noguchi and M. Miyayama, *Appl. Phys. Lett.*, 93, 242903 (2008).
26) S. Teranishi, M. Suzuki, Y. Noguchi, M. Miyayama, C. Moriyoshi, Y. Kuroiwa, K. Tawa and S. Mori, *Appl. Phys. Lett.*, 92, 182905 (2008).
27) J. A. Zvirgzds, P. P. Kapostis and J. V. Zvirgzde, *Ferroelectrics*, 40, 75–77 (1982).
28) I. G. Siny, C.-S. Tu and V. H. Schmidt, *Phys. Rev. B*, 51, 5659–5665 (1995).
29) G. O. Jones and P. A. Thomas, *Acta Crystallogr., Sect. B: Struct. Sci.*, 58, 168–178 (2002).
30) K. Sakata and Y. Masuda, *Ferroelectrics*, 5, 347–349 (1974).
31) Y. Hiruma, H. Nagata and T. Takenaka, *IEEE Trans. Ultrason. Ferroelectr. Freq. Control*, 54, 2493–2499 (2007).
32) Y. Hiruma, K. Yoshii, H. Nagata and T. Takenaka, *J. Appl. Phys.*, 103, 084121 (2008).
33) T. Takenaka, A. Hozumi, T. Hata and K. Sakata, *Silic. Ind.*, 7, 136–139 (1993).
34) Y. Masuda, *Jpn. J. Appl. Phys.*, 33, 5549–5554 (1994).
35) T. Tsurumi, *J. Ceram. Soc. Japan*, 115, 17–22 (2007).
36) T. Tsurumi, Y. Kumano, N. Ohashi, T. Takenaka and O. Fukunaga, *Jpn. J. Appl. Phys.*, 36, 5970–5975 (1997).
37) N. Yanase, K. Abe, N. Fukushima and T. Kuwakubo, *Jpn. J. Appl. Phys.*, 38, 5305–5308 (1999).
38) Y. Nakano, T. Nomura and T. Takenaka, *Jpn. J. Appl. Phys.*, 42, 6041–6044 (2003).
39) Y. Nakano, T. Nomura and T. Takenaka, *Jpn. J. Appl. Phys.*, 43, 5398–5403 (2004).
40) R. E. Newnham, A. Dogan, Q. C. Xu, K. Onitsuka, J. Tressler and S. Yoshikawa, *Ultrasonic Symposium*, 509–513 (1993).
41) K. Uchino, "Piezoelectric Actuators and Ultrasonic Motors," Kluwer Academic Publishers.
42) K. Motoo, N. Toda, T. Fukuda, F. Arai, K. Kikuta, S. Hirano and T. Matsuno, *Proc. of the Robot Society of Japan*, **24**, 1A21 (2006).
43) K. Uchino, *Acta Mater.*, 46, 3745–3753 (1998).